

## SPINES AND TOPOLOGY OF THIN RIEMANNIAN MANIFOLDS

STEPHANIE B. ALEXANDER AND RICHARD L. BISHOP

**ABSTRACT.** Consider Riemannian manifolds  $M$  for which the sectional curvature of  $M$  and second fundamental form of the boundary  $B$  are bounded above by one in absolute value. Previously we proved that if  $M$  has sufficiently small inradius (i.e. all points are sufficiently close to the boundary), then the cut locus of  $B$  exhibits canonical branching behavior of arbitrarily low branching number. In particular, if  $M$  is *thin* in the sense that its inradius is less than a certain universal constant (known to lie between .108 and .203), then  $M$  collapses to a triply branched simple polyhedral spine.

We use a graphical representation of the stratification structure of such a collapse, and relate numerical invariants of the graph to topological invariants of  $M$  when  $B$  is simply connected. In particular, the number of connected strata of the cut locus is a topological invariant. When  $M$  is 3-dimensional and compact,  $M$  has complexity 0 in the sense of Matveev, and is a connected sum of  $p$  copies of the real projective space  $P^3$ ,  $t$  copies chosen from the lens spaces  $L(3, \pm 1)$ , and  $\ell$  handles chosen from  $S^2 \times S^1$  or  $S^2 \tilde{\times} S^1$ , with  $\beta$  3-balls removed, where  $p + t + \ell + \beta \geq 2$ . Moreover, we construct a thin metric for every graph, and hence for every homeomorphism type on the list.

### 1. INTRODUCTION

Our program for extracting topological constraints from geometric bounds is as follows [AB1, AB2]. We have proved that if a Riemannian manifold  $M$  with nonempty boundary  $B$  has sufficiently small inradius relative to curvature, then the cut locus of  $B$  exhibits canonical branching behavior of arbitrarily low branching number [AB2]. Therefore  $M$  is forced by geometric bounds to collapse to a polyhedron with certain canonical singularities. This establishes a connection between global Riemannian geometry and the notion in PL-topology of collapse to a simple polyhedral spine. In particular, a class of spines that was studied by Fet and Lagunov in the 1960's [LF1] but since has received little attention is seen to be natural in the Riemannian setting. We examine the topological consequences of collapse to such a spine.

For example, the following topological classification of thin Riemannian 3-manifolds will be an application of our work. Here  $\rho_k = (1/2) \log(2k/k + 1)$ , the radius of the largest ball centrally located between  $(k + 1)$  pairwise tangent horospheres in  $H^k$ . We conjecture that the universal constant  $\tilde{a}_{33}$  equals  $\rho_3$  (see §2).

---

Received by the editors June 4, 2001 and, in revised form, July 12, 2002.

2000 *Mathematics Subject Classification.* Primary 53C21, 57M50.

*Key words and phrases.* Riemannian manifolds with boundary, collapse, 3-manifolds, curvature bounds, inradius, stratification.

**Theorem 1.1.** *Let  $M$  denote a compact, connected Riemannian 3-manifold with simply connected boundary  $B$ , satisfying  $|K_M| \leq 1$  and  $|II_B| \leq 1$ , where  $K_M$  is sectional curvature of the interior and  $II_B$  is the second fundamental form of the boundary. There is a universal constant  $\tilde{a}_{33}$ , where  $.108 < \tilde{a}_{33} \leq \rho_3 \approx .203$ , such that if the inradius of  $M$  is less than  $\tilde{a}_{33}$ , then  $M$  has the following homeomorphism type: a connected sum of  $S^3$  with  $p$  copies of the real projective space  $P^3$ ,  $t$  copies chosen from the lens spaces  $L(3, \pm 1)$ , and  $\ell$  handles chosen from  $S^2 \times S^1$  or  $S^2 \tilde{\times} S^1$ , the twisted  $S^2$  bundle over  $S^1$ , with  $\beta$  3-balls removed, where  $p + t + \ell + \beta \geq 2$ . Every such homeomorphism class can be realized, with inradius arbitrarily close to (but larger than)  $\rho_2 \approx .144$ .*

Fet and Lagunov [LF2] constructed a domain  $M$  in  $\mathbf{R}^3$  whose boundary is a 2-sphere with  $|II_B| \leq 1$ , and whose inradius is arbitrarily close to  $\sqrt{3/2} - 1 \approx .225$  (the radius of the largest ball centrally located between four pairwise tangent unit spheres in  $\mathbf{R}^3$ ). An analogous construction in  $H^3$  yields a domain  $M$  with  $K_M = -1$ ,  $|II_B| \leq 1$ , and inradius arbitrarily close to but larger than  $\rho_3$ . In these examples,  $M$  is homeomorphic to  $S^3$  with a 3-ball removed, so  $p + t + \ell + \beta = 1$  and  $M$  does not satisfy the conclusion of Theorem 1.1. It follows that  $\tilde{a}_{33} \leq \rho_3$ . It can be shown that the spine in these examples is Bing's "house with two rooms" (illustrated in [RS, p.2]). This spine has two points with branching number 4 and hence is not triply branched.

The proof of Theorem 1.1 exploits the fact that the cut locus of  $B$  is a triply branched simple polyhedral spine. This is the critical case for 3-manifolds, since theorems of Weinstein and Buchner [W, B] imply that there is no topological restriction on an  $n$ -dimensional Riemannian manifold ( $n > 2$ ) with spherical boundary and  $(n + 1)$ -branched simple polyhedral cut locus.

The first Riemannian classification theorem of the type of Theorem 1.1 was due to Gromov [G, Th. V]. That theorem gives a bound on normalized inradius that forces an  $n$ -dimensional Riemannian manifold to be either the product of a manifold without boundary and an interval, or doubly covered by such. This is the case of the doubly branched spine (in our notation below, the case  $k = 2$ ; in this paper, we study the case  $k = 3$ ). The forcing inradius in [G] is on the order of  $n^{-n^n}$ . In [AB1], the existence of a dimension-independent forcing inradius  $\tilde{a}_2 > .075$  was established.

The proof of Theorem 1.1 involves classifying up to homeomorphism the compact 3-manifolds with triply branched simple polyhedral spines and simply connected boundary (Theorem 4.1 below). Here we make contact with Matveev's complexity theory of closed 3-manifolds [Ma2, Ma3], and our description of the class of manifolds involved follows from his work. We go beyond giving just the homeomorphism type, by showing that the 3-manifolds on the list all admit our more restrictive type of spine, and by accounting for all possible decompositions into simple blocks glued together along annuli. Moreover, we construct thin Riemannian metrics for all manifolds on the list.

As an important tool, we identify graphical representations of such a spine structure in arbitrary dimension. An exception occurs in dimension 4.

Finally, in arbitrary dimension, we study numerical invariants of manifolds with simply connected boundary that collapse to triply branched simple polyhedral spines, and hence of Riemannian  $n$ -manifolds with curvature and inradius bounds as in Theorem 1.1. An unexpected consequence is that for any such Riemannian

metric, the number of connected strata of each dimension in the cut locus of the boundary is a topological invariant of the underlying manifold, even though these strata may be arranged in many geometrically distinct ways (§6).

## 2. THIN RIEMANNIAN MANIFOLDS

**2.1. Forcing inradius.** Let  $M$  denote a complete  $n$ -dimensional Riemannian manifold with boundary  $B$ . The *inradius*,  $\mathcal{I}nr$ , of  $M$  is the supremum of the distance to  $B$ . The scale-free invariant  $\mathcal{I}nr \cdot \max\{\sup \sqrt{|K_M|}, \sup |\Pi_B|\}$  is called the *normalized inradius* of  $M$ . We study manifolds with small normalized inradius:

**Theorem 2.1** ([AB2]). *There exists a sequence of positive universal constants  $0 < \tilde{a}_2 \leq \tilde{a}_3 \leq \dots$  (independent of the dimension  $n$ ), such that if  $M$  has normalized inradius less than  $\tilde{a}_k$ , then the cut locus of the boundary  $B$  is a  $k$ -branched simple polyhedron of dimension  $n - 1$ , and is a spine of  $M$ . (If  $k > n + 1$ , we mean here that the cut locus is  $(n + 1)$ -branched.) Here  $\tilde{a}_2 > .075$  and  $\tilde{a}_3 > .108$ .*

Recall that a *cut point* of  $B$  is either a point in  $M$  with more than one minimizer to  $B$ , or a focal point of  $B$ . The universal constant  $\tilde{a}_k$  may be defined to be the infimum of normalized inradii of complete Riemannian manifolds having a cut point at which the angle between some pair of minimizers to  $B$  is less than or equal to  $\cos^{-1}(-1/k)$ . Note that  $\cos^{-1}(-1/k)$  is the central angle subtended by a vertex pair of a regular  $k$ -simplex. The example of a disk of radius  $\pi/4$  in the standard unit 2-sphere immediately shows that  $\tilde{a}_k < \pi/4$  for all  $k$ , since the boundary has  $|\Pi_B| = 1$  and the center point is a focal point of  $B$  at which the angle between a pair of minimizers to  $B$  may be chosen arbitrarily. Since all our inradius bounds will be less than  $\pi/4$ , it follows from standard Jacobi field comparisons that focal points will never occur in our setting.

If  $M$  has normalized inradius less than  $\tilde{a}_k$ , then by the proof of Theorem 2.1, from any given cut point there are  $r \leq k$  minimizers to  $B$ , and their initial unit tangent vectors  $u_1, \dots, u_r$  satisfy the condition that  $u_1 - u_2, \dots, u_1 - u_r$  are linearly independent. (In particular,  $r \leq n + 1$ . This means that if  $M$  has normalized inradius less than  $\lim_{k \rightarrow \infty} \tilde{a}_k$ , then there are at most  $n + 1$  minimizers from any cut point and their initial unit tangents are affinely independent.) It follows that the cut locus is a  $k$ -branched simple polyhedral spine (see below) and  $M$  collapses to  $C$  along the minimizers.

Holding the dimension  $n$  of  $M$  fixed in the above definition of  $\tilde{a}_k$  yields the constants  $\tilde{a}_{kn}$  for all  $n \geq k$ . These constants are increasing in  $k$  by definition, and decreasing in  $n$ , as may be seen by taking cartesian products with a line. Thus  $\tilde{a}_{kn} \downarrow \tilde{a}_k$ . As mentioned in the Introduction, an important feature of Theorem 2.1 is that the limits  $\tilde{a}_k$  are strictly positive.

Indeed, we have an algorithm for generating a strictly increasing sequence  $a_k$  satisfying  $0 < a_k \leq \tilde{a}_k$ , with  $a_2 \approx .075$  and  $a_3 \approx .108$ . In spite of the difficulty of establishing these bounds, we know of no counterexample to the conjecture that  $\tilde{a}_{kn} = \tilde{a}_k = \rho_k$  for  $n \geq k$ , where  $\rho_k$  is the hyperbolic interstitial radius defined in §1. An upper bound for the  $\rho_k$  is  $\log 2/2 \approx .347$ , whereas our constants  $a_k$  increase to .195. Examples showing  $\rho_k \geq \tilde{a}_{kk} \geq \tilde{a}_k$  are constructed in the next subsection. For  $k = 2, 3$ , one may take ‘‘Swiss cheeses’’ in  $H^k$  with horoballs as holes. In particular, our constants  $a_2$  and  $a_3$  are sharp to within a factor of 2.

Starting with §3, this paper focuses on manifolds with triply branched simple polyhedral spines (as defined below). Thus we define a *thin* Riemannian manifold with boundary to be one whose normalized inradius is less than  $\tilde{a}_3$ .

**2.2. Examples.** Here we show  $\tilde{a}_{kk} \leq \rho_k$ , by constructing a  $k$ -dimensional manifold  $M$  with  $|K_M| \leq 1$ ,  $|\text{II}_B| \leq 1$ , inradius arbitrarily close to  $\rho_k$ , and such that the angle between some pair of minimizers to  $B$  is less than or equal to  $\cos^{-1}(-1/k)$ .

For  $k = 2, 3$ , consider  $k + 1$  pairwise tangent horoballs in  $H^k$ . Their centers at infinity determine a regular ideal  $k$ -simplex. The group  $G$  generated by reflections in its  $(k - 1)$ -faces yields a tessellation by regular ideal  $k$ -simplices, and a corresponding packing of  $H^k$  by horoballs. The desired manifold  $M$  is obtained by shrinking all the horoballs by an arbitrarily small fixed amount and removing their interiors. Then the inradius of  $M$  is arbitrarily close to  $\rho_k$ . At any point having  $k + 1$  minimizers to  $B$ , some pair of the  $k + 1$  initial tangents has angle less than or equal to  $\cos^{-1}(-1/k)$  ([AB2, Lemma 2.2]). Compact examples may be obtained as quotients under subgroups of  $G$  [Th, p. 129].

The same construction fails for  $k > 3$ , because the images under  $G$  of the original  $k + 1$  horoballs overlap. This assertion follows from the analogous one for  $k$  pairwise tangent Euclidean balls of fixed radius in  $\mathbf{R}^{k-1}$ . The reduction is by taking one of the horospheres to be  $x^k = 1$  in the upper halfspace model of  $H^k$ , so that the remaining  $k$  horospheres are Euclidean spheres tangent to  $x^k = 1$  and  $x^k = 0$ . The subgroup of  $G$  generated by reflections in the vertical  $(k - 1)$ -faces stabilizes the horosphere  $x^k = 1/2$ , and its action there is generated by Euclidean reflections in the  $(k - 2)$ -faces of the corresponding Euclidean  $(k - 1)$ -simplex.

Now we give a construction that works for all  $k$ . Again start with  $k + 1$  pairwise tangent horoballs in  $H^k$ . Rolling a horosphere  $H$  around this configuration envelops it by a hypersurface  $\tilde{B}$  that satisfies  $|\text{II}_{\tilde{B}}| \leq 1$ , except at certain singular loci where  $\tilde{B}$  is merely  $C^1$ . The desired manifold  $M$  is obtained by shrinking the original  $k + 1$  horospheres by an arbitrarily small amount and removing their interiors from the region bounded by  $\tilde{B}$ , as illustrated in Figure 1(a) for  $k = 2$ . The balls that realize the inradius of  $M$  are centered at cut points having  $k + 1$  minimizers to the boundary, and so as before some pair of minimizers has angle less than or equal to  $\cos^{-1}(-1/k)$ . Since the singular loci of  $\tilde{B}$  are away from these balls, scaling by  $1 + \epsilon$  and smoothing produces smooth examples  $M$  with the desired properties.

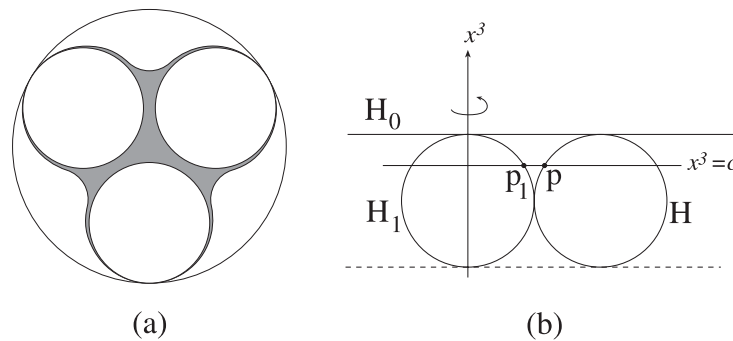


FIGURE 1.

The key claim to check is  $|\Pi_{\tilde{B}}| \leq 1$ . We examine the portion of  $\tilde{B}$  that is swept out when the rolling horosphere  $H$  touches exactly  $r$  of the original horospheres, say  $H_0, \dots, H_{r-1}$ ,  $1 \leq r \leq k$ . Taking  $H_0$  to be  $x^k = 1$  in the upper halfspace model, we see that the envelope swept out by  $H$  is obtained by moving a generating regular  $(r-1)$ -simplex of  $H$  along either a punctured regular  $(k-1)$ -simplex in  $H_0$  if  $r = 1$ , or a regular  $(k-r)$ -simplex in a hypersphere of  $H_0$  if  $r > 1$ . To bound the normal curvatures of  $\tilde{B}$  in a direction lying in the  $(k-r)$ -dimensional subspace orthogonal to a generator, it suffices by symmetry to examine the case  $k = 3, r = 1$ . Consider the intersection curves of the horosphere  $x^3 = c$  with  $\tilde{B}$  and  $H_1$  respectively. In Figure 1(b), these are the curves swept out by  $p$  and  $p_1$  under the indicated rotation. In the horosphere  $x^3 = c$ , whose intrinsic and model geometries are homothetic, the inward normal curvature vector of the first curve is no greater than that of the second. By symmetry, the length of the projection of the first vector on the normal to  $\tilde{B}$  is no greater than that of the second vector on the normal to  $H_1$ , namely, 1.

Using methods similar to those in §5, one may also obtain compact examples by truncating those just constructed and gluing after metric modification.

### 3. SPINES

**3.1. Simple polyhedral spines.** This class of spines was introduced in [Ma1]. The definitions of *k-branched simple polyhedral spine* and *collapse* are reviewed in [AB2]; when using these terms we always refer to the category of polyhedra and piecewise-linear maps. In this paper we only consider triply branched spines, and now we set out what is needed in that setting.

A *triply branched simple (n-1)-dimensional polyhedron*  $C = C_2 \cup C_3$  is stratified by its  $(n+1-r)$ -dimensional submanifolds  $C_r$ ,  $r = 2, 3$ . Every  $p \in C_3$  has a neighborhood in  $C$  that is PL homeomorphic to the product of  $I^{n-2}$  with a cone over three points (say with cone point  $v$ ), where  $I = [-1, 1]$  and  $p$  corresponds to  $v \times \{(0, \dots, 0)\}$ .

Suppose  $M$  is a PL manifold with boundary  $B$ , and  $C$  is embedded as a closed subset of the interior of  $M$ . We say  $M$  *collapses to*  $C$ , and  $C$  is a *spine* of  $M$ , if there is a map  $\Phi : B \times [0, 1] \rightarrow M$  whose restriction to  $B \times [0, 1)$  is a homeomorphism onto  $M - C$ , and whose restriction  $\Phi_1$  to  $B = B \times \{1\}$  has image  $C$ . Then since  $\Phi$  is PL,  $\Phi$  acts as an imbedding on the product of some neighborhood of each point in  $B$  with  $[0, 1]$ . See the discussion in [Ma1]. In particular, if  $p \in C_r$ ,  $r = 2, 3$ , then  $\Phi_1^{-1}(p)$  consists of exactly  $r$  points of  $B$ .  $B$  is stratified by the manifolds  $B_r = \Phi_1^{-1}(C_r)$ , where  $B_r$  is an  $r$ -fold cover of  $C_r$ . By a *diod stratum* of  $C$  or  $B$ , we mean a component of  $C_2$  or  $B_2$  respectively, and by a *triod stratum*, a component of  $C_3$  or  $B_3$ .

For example, suppose  $M$  is 3-dimensional and compact, so that the triod strata are circles. The *triod block* in Figure 2, with its two ends identified, illustrates a neighborhood in the spine  $C$  of a triod stratum, together with the points of  $M$  that collapse to it. The identification of the ends is by translation, translation and rotation through  $2\pi/3$ , or translation and reflection through one of the central rectangles. The shaded portion of the boundary of the block (after identification of the ends) lies in  $B$ . The unshaded portion represents one, two or three annular gluing seams along which the block is attached to its complement in  $M$ .

Theorem 2.1 relates the cut locus of the boundary of a Riemannian manifold to collapse. Namely, if  $M$  has normalized inradius less than  $\tilde{a}_k$ , then each cut

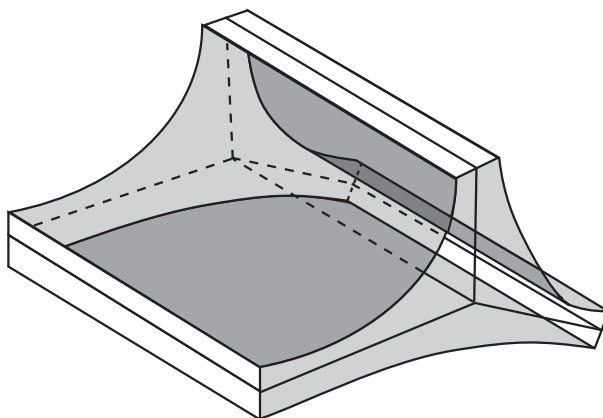


FIGURE 2.

point has at most  $k$  minimizers to  $B$ , and the cut locus  $C$  is a  $k$ -branched simple  $(n - 1)$ -dimensional polyhedron.  $M$  collapses to  $C$  along the minimizers.

**3.2. Holonomy of spines.** Suppose an  $n$ -dimensional PL manifold  $M$  with boundary  $B$  collapses to a triply branched simple polyhedral spine  $C$ , via the map  $\Phi : B \times [0, 1] \rightarrow M$ . Corresponding to the 3-fold covering of a triod stratum  $C_{3i}$  of  $C$  by strata in  $B$ , we have a triod bundle over  $C_{3i}$ , whose fiber at  $p$  consists of the cone over the 3 points of  $B$  that collapse to  $p$ . Moving around a loop in  $C_{3i}$  yields a permutation of the fiber, either the identity, a cyclic permutation or a transposition (as in Figure 2, where the two ends are respectively identified by a translation, translation and rotation through  $2\pi/3$ , or translation and reflection through a central rectangle).

Thus we obtain an induced homomorphism of the fundamental group  $\pi_1(C_{3i})$  to the permutation group  $S_3$ . Its image is the *holonomy group* of the stratum  $C_{3i}$ .

The following key fact allows us to transfer topological information from  $B$  to  $M$ . It states that transposition holonomy does not occur when  $H_1(B, \mathbf{Z}_2) = 0$ .

**Proposition 3.1** ([AB2]). *Suppose a manifold  $M$  collapses to a triply branched simple polyhedral spine. If  $H_1(B, \mathbf{Z}_2) = 0$ , then each triod stratum of the spine is orientable, and its holonomy group is either the identity or the alternating subgroup of  $S_3$ .*

**3.3. Graphical representation of stratifications.** Suppose a manifold  $M$  collapses to a triply branched simple polyhedral spine. Now we describe a graphical coding of the corresponding stratifications of the spine  $C$  and boundary  $B$  of  $M$ .

The *spine graph*  $c$  is a bipartite graph whose vertices  $c_{3i}$  and  $c_{2j}$  represent the triod and diod strata  $C_{3i}$  and  $C_{2j}$ , respectively, of the spine  $C$ . The edges adjacent to a triod vertex  $c_{3i}$  represent the components into which  $C_{3i}$  separates a normal neighborhood of itself in  $C$ . Each such component lies in some diod stratum  $C_{2j}$ , and the edge representing that component joins  $c_{3i}$  to  $c_{2j}$ . A diod stratum  $C_{2j}$  is homeomorphic to the interior of a connected  $(n - 1)$ -dimensional manifold with boundary having a natural map, not necessarily one-one, onto the closure of  $C_{2j}$  in  $C$ . The boundary components of this manifold with boundary are in one-one correspondence with the edges adjacent to the diod vertex  $c_{2j}$ .

The *boundary graph*  $b$  is a bipartite graph whose vertices  $b_{3i'}$  and  $b_{2j'}$  represent the triod and diod strata  $B_{3i'}$  and  $B_{2j'}$  of  $B$ . The edges adjacent to a triod vertex  $b_{3i'}$  represent the components into which  $B_{3i'}$  separates a small tubular neighborhood of itself in  $B$ . Each such component lies in some  $B_{2j'}$ , and the edge representing that component joins  $b_{3i'}$  to  $b_{2j'}$ .

The pair  $(b, c)$  is equipped with a simplicial projection  $\varphi : b \rightarrow c$  corresponding to the action of the map  $\Phi_1 : B \rightarrow C$ , which maps each stratum of the boundary onto a stratum of the spine. We now show that under the assumption  $H_1(B, \mathbf{Z}) = 0$ , the graph pairs are obtained by gluing together configurations of only four types, shown in Figure 3 (a)-(d). (Without this assumption on the boundary, another configuration is possible, corresponding to transposition holonomy; see [AB2, Remark 4.6].)

Our figures use the following convention: *Diod vertices are light, triod vertices are dark, boundary graphs are shaded, and the projection map  $\varphi$  is indicated by proximity.*

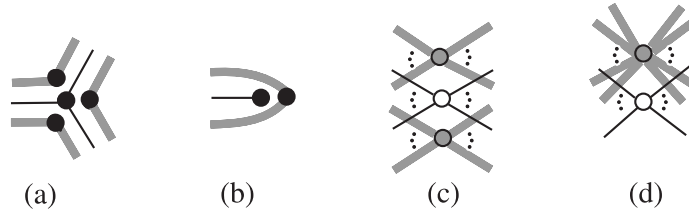


FIGURE 3.

**Proposition 3.2.** *Suppose an  $n$ -dimensional manifold  $M$  with boundary  $B$  collapses to a triply branched simple polyhedral spine, and  $H_1(B, \mathbf{Z}) = 0$ . Then the corresponding graph pair  $(b, c)$  has the following properties:*

- (1) *Figures 3 (a) and (b) are the only admissible configurations for a neighborhood of a triod vertex in  $c$  and its preimage in  $b$ .*
- (2) *Figures 3 (c) and (d) (where the number of edges in the spine graph configuration is  $e \geq 0$ , and the number of edges in the boundary graph configuration is  $2e$ ) are the only admissible configurations for a neighborhood of a diod vertex in  $c$  and its preimage in  $b$ .*
- (3) *The components of  $b$  are trees.*

*Proof.* (1) Every triod stratum  $C_{3i}$  of the spine is triply covered by its  $\Phi_1$ -preimage, whose number of components is 3 or 1, according to whether the holonomy group of  $C_{3i}$  is the identity or the alternating subgroup of  $S_3$  respectively. Thus every triod vertex  $c_{3i}$  of the spine graph  $c$  has 3 or 1  $\varphi$ -preimages in the boundary graph. This multiplicity agrees with the valence of  $c_{3i}$ , by the isomorphism of the two triod bundles over  $C_{3i}$  that respectively represent  $\Phi_1^{-1}|_{C_{3i}}$  and the collar structure adjacent to  $C_{3i}$  in  $C$  [AB2, Proposition 3.1].

The assumption  $H_1(B, \mathbf{Z}) = 0$  implies that each triod stratum in  $B$  separates  $B$  into two components. Thus every triod vertex in the boundary graph  $b$  has valence 2. It follows from Proposition 3.1 that the action of  $\varphi$  on edges is as shown in Figure 3(a) and (b). This proves (1). Note that every edge of  $c$  has two preimages in  $b$ .

(2) Every diod stratum  $C_{2j}$  of the spine is doubly covered by its  $\Phi_1$ -preimage. Thus every diod vertex  $c_{2j}$  of  $c$  has 2 or 1 preimages in  $b$ , according to whether the covering is trivial or nontrivial, respectively. In the former case, the stars in  $b$  of the two preimages of  $c_{2j}$  are isomorphic. Since every edge of  $c$  has two preimages, (2) follows.

(3) Finally, it is proved in [AB2, Theorem 4.9] that if  $H_1(B, \mathbf{Z})$  is finite, then (3) holds.  $\square$

We define an *admissible graph pair*  $(b, c)$  by properties 1-3 of Proposition 3.2. The simplest admissible graph pairs (in a sense made precise in the next subsection) are shown in Figure 4. (Since every edge of a graph must join two vertices, the configurations of Figure 3 are not themselves graph pairs.)

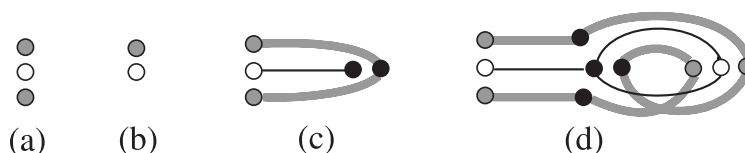


FIGURE 4.

Figure 4 (a) is realized by  $M = C \times I$  for any manifold  $C$  without boundary. Figure 4 (b) may be realized by taking  $M$  to be punctured  $P^n$  (i.e., with a ball removed), so that  $B = S^{n-1}$  and  $C = P^{n-1}$ . For 3-manifolds, Figure 4(c) is realized by the punctured lens space  $L_{(3,1)}$ , with  $C$  a disk whose boundary is triply wrapped. Figure 4(d) is realized by  $S^2 \times S^1$  or  $S^2 \tilde{\times} S^1$ , where  $C$  is  $T^2$  with an attached meridional disk.

Theorem 5.2 below shows how to realize any admissible graph pair.

**3.4. Combinatorial invariants.** Here is our list of primitive invariants of an admissible graph pair  $(b, c)$ ,

$$\begin{aligned} \ell &= \text{rank } H_1(c, \mathbf{Z}), \\ p &= \text{the number of diod vertices in } c \text{ of } \varphi\text{-multiplicity 1,} \\ t &= \text{the number of triod vertices in } c \text{ of } \varphi\text{-multiplicity 1,} \\ \gamma &= \text{the number of components of } c, \\ \beta &= \text{the number of components of } b. \end{aligned}$$

Figure 4 illustrates all the admissible graph pairs for which  $p + t + \ell + \beta = 2$ . We now give a simple combinatorial proof that this sum cannot be 1. A much more circuitous proof of this fact in the compact case follows from [LF1, Lemma 16] (see [AB2, Lemma 4.14]) and [AB2, Theorem 5.1]. We shall see below how to transform Proposition 3.3 into the statement that punctured  $S^3$  has no triply branched simple polyhedral spine (see [I, Lemma 4] for a more general statement). This is an example of an interesting phenomenon whereby, through coding by graph pairs, theorems about 3-manifolds can be used to prove theorems about  $n$ -manifolds.

**Proposition 3.3.** *For any admissible graph pair,  $p + t + \ell + \beta \geq 2$ .*

*Proof.* Suppose to the contrary that  $p + t + \ell + \beta < 2$ , so  $p = t = \ell = 0$  and  $\beta = 1$ .

The defining conditions (3) and (2) of an admissible graph pair (Proposition 3.2) imply that every admissible graph pair has at least one *end*. That is, either the entire graph pair is as shown in Figure 4(a) or (b), or a neighborhood of some diod vertex in the spine graph  $c$  and its preimage in the boundary graph  $b$  are as shown in Figure 5. Since we assume  $\beta = 1$  and  $p = 0$ , only the last case is possible.

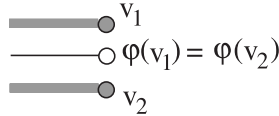


FIGURE 5.

Since the boundary graph  $b$  is connected, there is a path  $\sigma$  in  $b$  joining the two vertices  $v_1$  and  $v_2$  of  $b$  in the end. Since  $\varphi(v_1) = \varphi(v_2)$ , then  $\varphi(\sigma)$  is a loop in  $c$ . Without loss of generality, we may assume  $\sigma$  does not backtrack, that is, traverse any edge in one direction and then immediately in the opposite direction. The configuration of the graph pair at any vertex of  $b$  is as shown in Figure 3(a) or (c), since (b) is ruled out by the assumption  $t = 0$  and (d) is ruled out by the assumption  $p = 0$ . This means that  $\varphi(\sigma)$  also cannot backtrack. (By contrast, the presence of configuration (b) or (d) would allow backtracking of  $\varphi(\sigma)$ .) Therefore  $\varphi(\sigma)$  contains a nontrivial loop, in contradiction to the assumption  $\ell = 0$ .  $\square$

By Proposition 3.3 and [AB2, Theorem 5.1], we have

**Theorem 3.4.** *Suppose an  $n$ -dimensional manifold  $M$  with boundary  $B$  collapses to a triply branched simple polyhedral spine, and  $H_1(B, \mathbf{Z}) = 0$ . Then  $H_1(M, \mathbf{Z}) = \bigoplus_{\ell} \mathbf{Z} \oplus_p \mathbf{Z}_2 \oplus_t \mathbf{Z}_3$ , where  $p + t + \ell + \beta \geq 2$  and  $\beta$  is the number of components of  $B$ .*

#### 4. TOPOLOGICAL CLASSIFICATION OF THIN THREE-MANIFOLDS

In this section we consider the case  $n = 3$ . It turns out that compact 3-manifolds with triply branched simple polyhedral spines and simply connected boundary are classified up to homeomorphism and chirality considerations by their first homology, as given in Theorem 3.4.

For a manifold  $M$  of any dimension, with triply branched simple polyhedral spine  $C$  and  $H_1(B, \mathbf{Z}) = 0$ , the decomposition of the graph pair of  $M$  into the blocks shown in Figure 3 (a)-(d) corresponds to a decomposition of  $M$  into *triod blocks* and *diod blocks*. Specifically, choose a normal neighborhood in the spine of each triod stratum  $C_{3i}$ . The points of  $M$  that collapse to that neighborhood form a triod block (as in Figure 2). The diod blocks are the components of the complement of the union of the triod blocks. The blocks are glued, triod to diod, according to the pattern indicated by the graph pair, along gluing seams which are trivial diod (segment) bundles. In dimension 3, the results of this gluing can be classified up to homeomorphism.

By a *handle*, orientable or nonorientable, we mean  $S^1 \times S^2$  or  $S^2 \tilde{\times} S^1$ , respectively. Uniqueness theorems for the decomposition of a 3-manifold into irreducible summands and handles were proved by H. Kneser [K]. See also Haken [H], and Milnor, who gave the connected sum formulation [Mi]. We use the following convention in speaking of the *connected sum* of a finite collection of irreducible 3-manifolds and

handles. We assume an orientation on every orientable member of the collection. If every member is oriented, then their connected sum is well-defined and oriented. If at least one member is nonorientable, then their (unoriented) connected sum is well defined and nonorientable. In the first case, the summands are uniquely determined as oriented manifolds. In the second case, the irreducible summands are uniquely determined as unoriented manifolds, and the number of handles is also determined.

Matveev has studied the *complexity* of punctured closed 3-manifolds, defined as the minimum number of vertices in an *almost simple* spine [Ma2, Ma3]. In particular, complexity is additive on connected sums and invariant under removing 3-balls, and the irreducible manifolds of low complexity are classified [Ma2]. The classification is extended to a higher complexity bound in [MP]. Since a triply branched simple polyhedral spine is a special case of an almost simple spine with no vertices, our 3-manifolds have complexity 0 and the class identified in the following theorem is the same, except for the 3-ball, as Matveev's list of manifolds of complexity 0. Thus the following theorem is a corollary of Matveev's work (together with Theorem 3.4, which relates the numbers of the summands to the block types). However, in our setting there is a simple way to exhibit the decomposition explicitly, as we do in the following proof.

**Theorem 4.1.** *Let  $M$  be a compact, connected 3-manifold with  $\beta$  spherical boundary components and a triply branched simple polyhedral spine. Then  $M$  is the connected sum of  $p$  copies of  $P^3$ ,  $\ell$  copies of the handles  $S^2 \times S^1$  or  $S^2 \tilde{\times} S^1$ , and  $t$  copies of the lens spaces  $L(3, \pm 1)$ , with  $\beta$  3-balls removed, where  $p, \ell$  and  $t$  are the previously defined invariants of the graph pair.*

*Proof.* Define  $M^+$  by filling in the boundary components of  $M$  with 3-balls. Then  $M^+ = M \cup_{1 \leq j \leq \beta} D_j^3$ , where  $D_j^3$  is a 3-ball and  $\bigcup_{1 \leq j \leq \beta} \partial D_j^3 = B$ .

Since  $M$  is 3-dimensional, the triod strata of the spine and the boundary of  $M$  are circles. By Proposition 3.1, the holonomy group of such a circle in the spine is either the identity or the alternating subgroup of  $S_3$ ; we say the holonomy is the identity or *cyclic*. The triod blocks are equivalent to the 3-dimensional Euclidean block in Figure 2 with its two ends identified by translation (identity holonomy), or rotation by angle  $2\pi/3$  (cyclic holonomy). The unshaded surfaces represent three or one annuli, respectively, along which the triod block is glued to its adjacent diod blocks.

The diod blocks are segment bundles, either trivial or nontrivial according to whether that diod stratum of the spine is trivially or nontrivially covered by its preimage in  $B$ . Since  $B$  is a union of 2-spheres, each component of the cover is a 2-manifold with boundary contained in  $S^2$ , and hence is  $S^2$  with some disks removed. Since the gluing seam between a triod block and a diod block is an annulus, the bundle structure is trivial on the boundary circles. Filling by trivial segment bundles over disks gives a double covering by  $S^2$ . Therefore a diod block either is the trivial segment bundle over the complement of disjoint 2-disks in  $S^2$ , or is the complement in the nontrivial segment bundle over  $P^2$  of some trivial segment bundles over disjoint 2-disks.

$M$  is constructed by gluing together finitely many blocks  $M_\alpha$  along annular gluing seams. Each  $M_\alpha$  is a triod block which has either identity or cyclic holonomy, or a diod block which is either a trivial or nontrivial segment bundle as just described. Each gluing is between a triod and a diod block. The boundary  $\partial M_\alpha$  is the union of  $\partial M_\alpha \cap B$  and annular gluing seams that lie, except for their boundary circles,

in the interior of  $M$ . Denote by  $B_k$  the components of  $\partial M_\alpha \cap B$  for all  $M_\alpha$ . Thus  $B = \bigcup B_k$ , and  $\bigcup_k \partial B_k = \bigcup_i C_i$ , where the  $C_i$  are the mutually disjoint circles in  $B$  that bound the annular gluing seams.

Each circle  $C_i$  may be filled by a 2-disk  $D_i^2$  lying in the filling 3-ball  $D_j^3$  on whose boundary  $C_i$  lies. The disks  $D_i^2$  may be taken to be mutually disjoint, so that they decompose  $\bigcup_j D_j^3$  into solids  $E_k^3$ , each of which is itself a 3-ball. Each  $E_k^3$  lies in a filling 3-ball  $D_j^3$  and satisfies  $E_k^3 \cap \partial D_j^3 = B_k$ .

For each block  $M_\alpha$ , define the extended block  $M_\alpha^+$  as follows: along each component  $B_k$  of  $\partial M_\alpha \cap B$ , glue to  $M_\alpha$  the corresponding solid  $E_k^3$ .

*Step 1.* We show that each extended block  $M_\alpha^+$  is the complement of finitely many 3-balls in one of  $S^3$ ,  $P^3$  or  $L(3, \pm 1)$ . Moreover, the boundary 2-spheres of  $M_\alpha^+$  are in one-one correspondence with the annular gluing seams on  $\partial M_\alpha$ . Each of these boundary 2-spheres consists of an annular gluing seam together with the two 2-disks  $D_i^2$  that fill its two boundary circles  $C_i$ . (Since the  $C_i$  may lie on different components of  $B$ , the  $D_i^2$  may lie in different filling 3-balls.)

(a)  $M_\alpha =$  triod block with identity holonomy. In this case, as is clear from Figure 2,  $M_\alpha$  is topologically a solid torus and  $\partial M_\alpha$  is the union of six parallel annuli, each homotopic to a loop that generates  $\pi_1(M_\alpha)$ . Three of these annuli are gluing seams (unshaded in Figure 2). They are separated alternately by the other three annuli, each of which is a component  $B_k$  of  $\partial M_\alpha \cap B$ . We obtain  $M_\alpha^+$  from  $M_\alpha$  by gluing, along each of these three annuli  $B_k$ , its corresponding solid  $E_k^3$ , which lies in a filling 3-ball  $D_j^3$  and satisfies  $E_k^3 \cap \partial D_j^3 = B_k$ . Here  $E_k^3$  is bounded by  $B_k$  and the two 2-disks  $D_i^2$  that fill its boundary circles. Thus  $E_k^3 = D^2 \times I$ , and the extended block  $M_\alpha^+$  is a 3-sphere with three 3-balls deleted. Each boundary 2-sphere of  $M_\alpha^+$  consists of one of the annular gluing seams of  $\partial M_\alpha$ , together with the two 2-disks  $D_i^2$  that fill its boundary circles.

(b)  $M_\alpha =$  triod block with cyclic holonomy. In this case,  $M_\alpha$  is again a solid torus, and  $\partial M_\alpha$  is the union of two parallel annuli, each homotopic to three times a loop that generates  $\pi_1(M_\alpha)$ . One annulus is a gluing seam, and the other annulus is  $B_k = \partial M_\alpha \cap B$ . As in (a),  $M_\alpha^+$  is obtained by gluing to the solid torus  $M_\alpha$ , along  $B_k$ , the solid  $E_k^3 = D^2 \times I$ . This operation yields a lens space  $L(3, 1)$  or  $L(3, -1) = L(3, 2)$  with one 3-ball deleted. (This construction coincides almost exactly with that for  $L(3, 2)$  in [Th, p. 39, Problem 1.4.7(b)].)

For a given orientation of  $M_\alpha$ , we distinguish between  $L(3, 1)$  and  $L(3, -1)$  according to whether the holonomy map is a  $2\pi/3$  rotation positively or negatively, respectively, with respect to a chosen direction of the base loop. This definition is independent of the choice of direction of the base loop.

(c)  $M_\alpha =$  trivial diod block. Here  $M_\alpha$  is the product of a segment and the 2-sphere with a finite number, say  $e_\alpha \geq 0$ , of disjoint 2-disks deleted (see Figure 6(a), which illustrates the case  $e_\alpha = 3$ ).  $\partial M_\alpha$  is the union of  $e_\alpha$  annular gluing seams and the two components  $B_k$  of  $\partial M_\alpha \cap B$ , where each  $B_k$  is a copy of the 2-sphere with  $e_\alpha$  disjoint 2-disks deleted (shaded in Figure 6(a)). We obtain  $M_\alpha^+$  from  $M_\alpha$  by gluing, along each of these two equivalent  $B_k$ , the solids  $E_k^3$ . For each of the two  $B_k$ , the corresponding solid  $E_k^3$  lies in a filling 3-ball, and is bounded by  $B_k$  and the  $e_\alpha$  2-disks  $D_i^2$  that fill the boundary circles of  $B_k$ . Gluing yields the extended block  $M_\alpha^+$  isomorphic to  $S^3$  with  $e_\alpha$  disjoint 3-balls deleted.

(d)  $M_\alpha =$  nontrivial diod block. Here  $M_\alpha$  is the complement, in the nontrivial segment bundle over the projective plane, of a finite number  $e_\alpha \geq 0$  of trivial

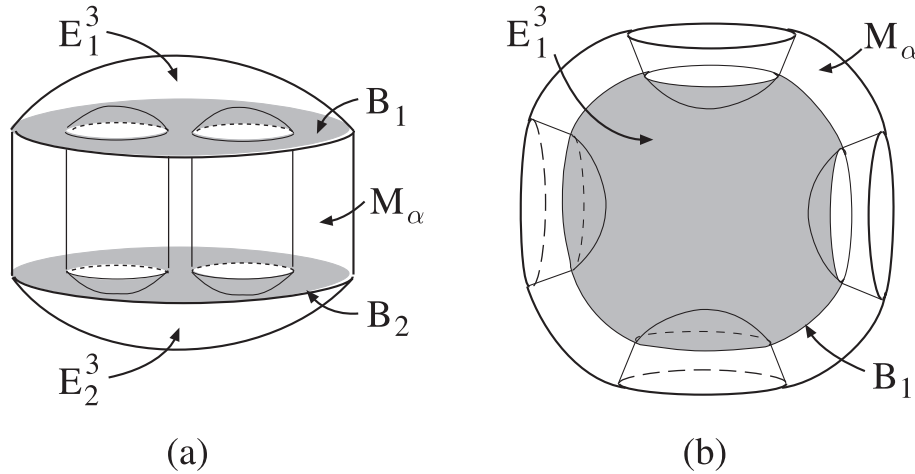


FIGURE 6.  $M_\alpha^+$

segment bundles over disjoint 2-disks. Recall that the nontrivial segment bundle over projective  $(n - 1)$ -space is projective  $n$ -space with an  $n$ -ball removed. Representing  $P^n$  by the closed  $n$ -ball with opposite points on the boundary identified, a visible model of the nontrivial segment bundle over  $P^{n-1}$  is obtained by removing a smaller central ball (as in Figure 6(b)). The segments of the bundle structure are then split into radial half-segments extending inward from the boundary.

Now  $\partial M_\alpha$  is the union of  $e_\alpha$  annular gluing seams together with  $B_k = \partial M_\alpha \cap B$ , where  $B_k$  is the 2-sphere with  $2m_\alpha$  disjoint 2-disks deleted (shaded in Figure 6(b), which represents the case  $e_\alpha = 2$ ). We obtain  $M_\alpha^+$  from  $M_\alpha$  by gluing, along  $B_k$ , the solid  $E_k^3$  bounded by  $B_k$  and the  $e_\alpha$  2-disks  $D_i^2$  that fill the boundary circles of  $B_k$ . Thus  $M_\alpha^+$  is  $P^3$  with  $e_\alpha$  disjoint 3-balls deleted.

*Step 2.* Since the blocks  $M_\alpha$  partition  $M$  and the solids  $E_k^3$  partition the filling 3-balls  $D_j^3$ , then the extended blocks  $M_\alpha^+$  partition  $M^+$ . Two extended blocks either have empty intersection, or else one is a triod block and one is a diod block and they intersect in one or more common boundary 2-spheres. Each such 2-sphere consists of a common annular gluing seam together with the two 2-disks  $D_i^2$  that fill its two boundary circles.

Thus  $M^+$  is the result of gluing the  $M_\alpha^+$  on pairs of boundary 2-spheres. The gluing pattern is represented by the graph pair. Specifically, the vertices  $v_\alpha$  of the spine graph  $c$  are in one-one correspondence with the blocks  $M_\alpha$ . Step 1 shows that the homeomorphism class of each  $M_\alpha^+$  can be read from the graph pair. This is because the block types (a)-(d) of Step 1 respectively correspond to the configurations (a)-(d) of Figure 3; in (c) and (d),  $e_\alpha$  is the valence of  $v_\alpha$  in  $c$ . An edge of  $c$  joining  $v_\alpha$  and  $v_\beta$  corresponds to the gluing of a pair of boundary 2-spheres of  $M_\alpha$  and  $M_\beta$  respectively.

Now choose a maximal tree  $T$  in  $c$ . Perform only the gluings represented by the edges of  $T$ , to obtain a 3-manifold  $N$ . Let  $N^+$  be obtained by filling in the remaining boundary 2-spheres of  $N$  by 3-balls. We may orient  $N^+$ , since all the  $M_\alpha^+$  are orientable and there are no loops in the gluing pattern for  $N$ . Thus we

have expressed  $N^+$  as the oriented connected sum of  $S^3$  with  $p$  copies of  $P^3$  and  $t$  summands chosen from copies of  $L(3, 1)$  and  $L(3, -1)$ .

The complement in  $c$  of  $T$  consists of  $\ell$  edges.  $M^+$  is therefore obtained by performing the  $\ell$  corresponding “auto-connected sums” on  $N^+$ . That is, pairs of boundary 2-spheres of  $N$  are identified. If all these identifications are orientation-reversing, then this operation of attaching handles is equivalent to taking the connected sum of  $N^+$  with  $\ell$  copies of  $S^2 \times S^1$  [Mi]. In this case,  $M^+$  is oriented and hence so is  $M$ .

If at least one identification is orientation-preserving, then  $M^+$  and  $M$  are nonorientable. Here there is no distinction between  $L(3, 1)$  and  $L(3, -1)$  summands, and the connected sum representation of  $M^+$  allows a free choice for the  $\ell$  handles of between 1 and  $\ell$  summands  $S^2 \tilde{\times} S^1$ , and the remaining ones  $S^2 \times S^1$ .  $\square$

*Remark 4.2.* Recall that an oriented manifold is defined to be *chiral* if there is no orientation-reversing self-homeomorphism. The opposite property is called *achiral*. Thus,  $S^3$  is achiral because its reflection in a central plane is such a homeomorphism. Similarly,  $P^3$  and  $S^2 \times S^1$  are achiral. On the other hand,  $L(3, 1)$  is chiral. That is,  $L(3, 1)$  and  $L(3, -1)$  are distinct as oriented manifolds; they are homeomorphic, but any such homeomorphism must reverse orientation ([K]; also see [ST, §77]).

It follows from Theorem 4.1 that the homeomorphism class of  $M$  is determined up to chirality considerations by its homology, and therefore also by its number of boundary components and its spine graph:

**Theorem 4.3.** *Let  $M$  be a compact, connected 3-manifold with spherical boundary components and a triply branched simple polyhedral spine. Then the homology  $H_1(M, \mathbf{Z}) = \bigoplus_{\ell} \mathbf{Z} \bigoplus_p \mathbf{Z}_2 \bigoplus_t \mathbf{Z}_3$  determines the homeomorphism class of  $M$  uniquely if  $M$  is nonorientable, and up to  $\lfloor \frac{t}{2} \rfloor + 1$  choices if  $M$  is orientable.*

*Proof.* For given values of the homology invariants  $\ell$ ,  $p$  and  $t$ , up to oriented homeomorphism, there are exactly  $t + 1$  oriented 3-manifolds  $M$  with those invariants. Namely,  $M^+$  is represented by a connected sum of  $\ell$  copies of  $S^2 \times S^1$ ,  $p$  copies of  $P^3$ ,  $k$  copies of  $L(3, 1)$ , and  $t - k$  copies of  $L(3, -1)$ , where  $k = 0, 1, \dots, t$ . Thus the number of homeomorphism classes of  $M$  is obtained by identifying pairs with opposite orientation, namely,  $\lfloor \frac{t}{2} \rfloor + 1$ .

If  $\ell = 0$ , then any  $M$  with homology invariants  $\ell, p$  and  $t$  is orientable. If  $\ell > 0$ , then there is exactly one nonorientable such  $M$ , represented by a connected sum of  $\ell$  copies of  $S^2 \tilde{\times} S^1$ ,  $p$  copies of  $P^3$ , and  $t$  copies of  $L(3, 1)$ .  $\square$

### 5. REALIZABILITY

In this section, we make good on the remaining unproved claim of Theorem 1.1, namely: “Every such homeomorphism class can be realized . . .”.

Recall that if an  $n$ -dimensional manifold  $M$  collapses to a triply branched spine and the first homology of the boundary of  $M$  vanishes, then the geometric structure of  $M$  is represented by an *admissible graph pair* (Proposition 3.2). We begin (Theorem 5.1) by proving the existence of an admissible graph pair with any given choice of the invariants  $p, t, \ell$  and  $\beta$  satisfying  $p + t + \ell + \beta \geq 2$ .

Then we analyze the realizability of admissible graph pairs by Riemannian manifolds of arbitrary dimension. In particular, we prove that any finite admissible

graph pair can be realized by a compact Riemannian 3-manifold  $M$  with the desired inradius bound (Theorem 5.2). By Theorem 4.1,  $M$  is homeomorphic to the connected sum of  $p$  copies of  $P^3$ ,  $\ell$  copies of the handles  $S^2 \times S^1$  or  $S^2 \tilde{\times} S^1$ , and  $t$  copies of the lens spaces  $L(3, \pm 1)$ , with  $\beta$  3-balls removed. Note that in general there are many graph pairs for a given choice of the invariants, and hence many geometric structures for a given homeomorphism class. For example, Figure 7 shows the four graph pairs with  $\ell = 1, p = 1, t = 0, \beta = 1$  and  $\gamma = 1$ .

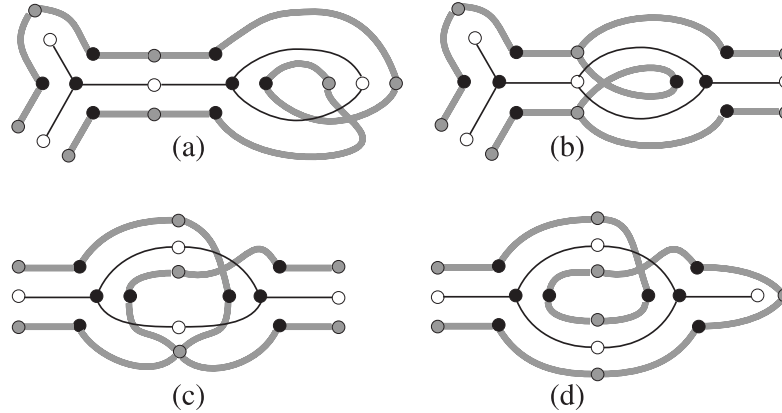


FIGURE 7.

**Theorem 5.1.** *There is an admissible graph pair with  $\gamma = 1$  and any given choice of the invariants  $p, t, \ell$  and  $\beta$  satisfying  $p + t + \ell + \beta \geq 2$ .*

*Proof.* Figure 4 shows the four admissible graph pairs that satisfy  $p + t + \ell + \beta = 2$ . The corresponding invariants  $(p, t, \ell, \beta)$  are respectively: (a)  $(0, 0, 0, 2)$ , (b)  $(1, 0, 0, 1)$ , (c)  $(0, 1, 0, 1)$ , and (d)  $(0, 0, 1, 1)$ . For any admissible graph pair  $(b, c)$ , there is at least one of these four basic pairs, all of whose invariants  $p, t, \ell, \beta$  are no greater than those of  $(b, c)$ . Thus it suffices to give operations on admissible graph pairs that independently increase each of the four invariants by 1.

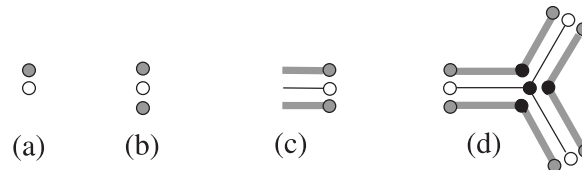


FIGURE 8.

The defining properties 3 and 2 (see Proposition 3.2) of an admissible graph pair imply that every such pair has at least one *end*. That is, either the pair is that of Figure 8(a) or (b), or the stars of some diod vertex in the spine graph  $c$  and its preimage in the boundary graph  $b$  are as shown in Figure 8(c). In either case, we construct a new admissible graph pair by attaching to an end the new block shown in Figure 8(d). The attaching of (d) to (b) or (c) is by identifying opposing diod vertices in the obvious way; and of (d) to (a), by identifying the opposing vertices

of the spine graphs, and identifying the single vertex of the boundary graph in (a) with both of the opposing vertices of the boundary graph in (d). The new graph pair has the same invariants  $p, t, \ell$  as the old one, and  $\beta$  increased by 1. It has one more end, with two ends located on the new block.

Now we “trade” this increase of 1 in  $\beta$  for an increase of 1 in any other invariant. Namely, to obtain a graph pair with the same  $t, \ell, \beta$  as the original and  $p$  increased by 1, modify one of the ends located on the new block (Figure 8(d)) by pinching together the two corresponding diod vertices of the boundary graph. The vertex is thus converted from type (c) to type (d) of Figure 3. To obtain the same  $p, \ell, \beta$  as the original and increase  $t$  by 1, attach, to one of the ends located on the new block, the block shown in Figure 4(c), by identifying end diod vertices in the obvious way. To obtain the same  $p, t, \beta$  as the original and increase  $\ell$  by 1, similarly attach, to one of the ends located on the new block, the block shown in Figure 4(d). These moves clearly retain the three defining properties.  $\square$

Now we are ready to prove our main realization theorem. It states that in any dimension except 4, any finite admissible graph pair may be realized by a compact Riemannian manifold with simply connected boundary. Moreover, the inradius may be made arbitrarily close to  $\rho_2$ . The first step is to verify the existence of a topological realization. Then we construct a corresponding Riemannian metric, namely, one for which the cut locus of the boundary is the given spine, and collapsing occurs along minimizers to the boundary.

The construction does not extend to dimension 4. Indeed, we show in Examples 5.4 and 5.5 below that in dimension 4, while some admissible graph pairs have topological realizations with spherical boundary components, others have no realization with  $H_1(B, \mathbf{Z}) = 0$ .

**Theorem 5.2.** *In any dimension  $n \neq 4$ , and for any finite admissible graph pair, there is a compact  $C^\infty$  Riemannian manifold with simply connected boundary, whose normalized inradius is arbitrarily close to  $\rho_2$ , and such that the cut locus of the boundary is a triply branched simple polyhedral spine realizing that graph pair. In dimension 3, every homeomorphism class described in Theorem 1.1 can be realized.*

*Proof.* It suffices to consider  $n = 3$ . Then for  $n \geq 5$ , one can take the product with the standard  $(n - 3)$ -dimensional sphere of radius 1.

First we show that any admissible graph pair has a topological realization as a 3-manifold  $M$  with simply connected boundary  $B$ . For vertices of type (a)-(d) of Figure 3, respectively, we use oriented triod or diod blocks of type (a)-(d) of Theorem 4.1, Step 1. The blocks are glued along annular gluing seams according to the pattern indicated by the graph pair.

In particular, each diod vertex  $b_{2j'}$  of the boundary graph  $b$  represents a diod stratum  $B_{2j'}$  of  $B$ , where  $B_{2j'}$  is a copy of  $S^2$  with a number of holes equal to the valence of  $b_{2j'}$ . Each edge adjacent to  $b_{2j'}$  joins it to a triod vertex of valence 2 (see Figure 3). This triod vertex represents a circle at which a boundary circle of  $B_{2j'}$  is glued to a boundary circle of another diod stratum; thus it corresponds to a connected sum operation. Since  $b$  is a tree, there are no auto-connected sums, and since all triod vertices of  $b$  have valence 2,  $B$  has empty boundary. Thus  $B$  is a union of 2-spheres.

The specific procedure for gluing the blocks is as follows. Each gluing corresponds to the identification of two annuli. This identification may be carried out in four

ways, depending on which pairs of boundary circles are identified (the *boundary circle choice*), and whether the identification reverses or preserves orientation (the *orientation choice*). The orientation choice is not represented on the graph pair, and hence may be made freely for the purpose of realizing a given graph pair, but not for realizing a homeomorphism class. The boundary circle choice is represented by the two ways of joining two pairs of half-edges in a boundary graph to make one pair of edges. (For example, in Figure 7(a), a change in this choice at the lower right would disconnect the boundary graph and destroy its tree property.)

Without loss of generality, we may assume the spine graph  $c$  is connected. Choose a maximal tree  $T$  in  $c$ . Perform the gluings corresponding to the edges of  $T$ , starting with one block and gluing each new block to the previous construction according to some sequential pattern. It is clear from Figure 3 that the resulting graph pair at each step is independent of the boundary circle choice. Now perform the gluings corresponding to some ordering of the  $\ell$  edges of  $c - T$ . At each step, the boundary circle choice is dictated by the components of the boundary graph already constructed (unless these components have symmetries that allow a free choice). Thus each admissible graph pair has a topological realization  $M$ .

To realize a given homeomorphism class for  $M$ , if  $M$  is nonorientable, then at least one identification of annuli must be orientation-preserving; if  $M$  is oriented, all must be orientation-reversing. Since moreover the orientation of each cyclic triod block may be freely chosen, it follows that every homeomorphism class in Theorem 1.1 can be realized.

Now we construct suitable Riemannian metrics on these diod and triod blocks, so that the gluing seams are totally geodesic and isometrically paired, and the gluings are smooth.

For all the triod blocks we use the same cross-section orthogonal to the central circle. Because of the exactness of the required lower bound  $\rho_2$  on the inradius, the construction has to be quite specific. A neighborhood of the center of that cross-section is a region of the hyperbolic plane  $H^2$  with curvature  $-1$ . We start with a horocycle  $\sigma$  in  $H^2$  and build a region based on  $\sigma$  (Figure 9), which will be  $1/6$  of the whole section (Figure 10). An arc between points  $p, q$  of  $\sigma$  will be part of the boundary; at  $q$  we continue the boundary curve to  $r$  by specifying a monotonic,  $C^\infty$  transition of the signed curvature of  $\sigma$  from 1 at  $q$  to 0 at  $r$ . The arclength along the boundary curve from  $q$  to  $r$  may be arbitrarily small, and is one of the parameters by which we will control the excess of the inradius over  $\rho_2$ .

From  $r$ , the boundary curve will continue along a geodesic segment. Now we modify the metric to the right of the perpendicular equidistant curve  $\lambda$  at  $r$ , by using a warped product metric instead of the hyperbolic metric. If  $t$  is the arclength along the geodesic segment in the boundary curve, such that  $t = 0$  occurs at the intersection with  $\lambda$ , then to the left, where  $t \leq 0$ , the metric of  $H^2$  has the representation  $ds^2 = dt^2 + \cosh^2(t - \tau) du^2$ . The parameter  $\tau > 0$  is free to choose, and  $\lambda$  will be given by  $t = 0$  in terms of these coordinates. For convenience we take  $u = 0$  as the equation of the geodesic continuation of the geodesic segment in the boundary curve. We continue to the right of  $\lambda$  by specifying the metric to be  $ds^2 = dt^2 + f^2 du^2$ , where the warping function  $f$  is a smooth convex extension of  $\cosh(t - \tau)$  for  $t \geq 0$ , which satisfies  $f'' \geq f$  and is a positive constant beyond some positive value of  $t$ . Then, by the curvature equation  $f'' + Kf = 0$ , the sectional curvature will pass from  $K = -1$  for  $t \leq 0$  to  $K = 0$  where  $f$  is constant.

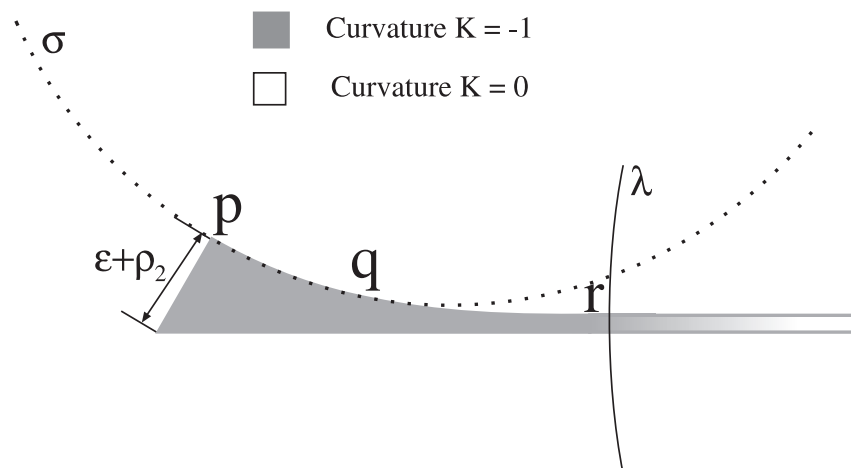


FIGURE 9.

Actually we have not yet specified the point  $p$  on  $\sigma$ ; we do so in conjunction with specifying the base line of the region. That base line is to be a horizontal geodesic  $u = u_0 < 0$  below the boundary geodesic. Each such horizontal geodesic forms an angle of  $\pi/3$  with a normal segment from one of its points to  $\sigma$ . If both  $u_0$  and the arclength from  $q$  to  $r$  are sufficiently close to 0, then the length of this normal segment is arbitrarily close to  $\rho_2$ . Indeed, by definition,  $\rho_2$  is the length of a normal segment to  $\sigma$  which makes an angle of  $\pi/3$  with a tangent line to  $\sigma$ .

Finally, we cut off the region to the right by a vertical segment in the region where  $K = 0$ . The construction of the complete triod cross-section is now simply a matter of reflecting the  $1/6$ -section alternately in the base and the line of the normal segment (see Figure 10). The inradius of this cross-section is  $\rho_2 + \epsilon$ , and the length of the three end segments is  $\delta = \delta(\epsilon)$ .

The triod block is completed by taking the Riemannian product of the cross section with an interval  $I$  whose length will be specified below, and identifying the two ends, either directly for a block with identity holonomy, or with a rotation of  $2\pi/3$  for a block with cyclic holonomy. Thus each gluing seam on a triod block is the product of a circle with an interval of length  $\delta$ .

The construction of suitable diod blocks is easier. For a given finite graph pair, there are finitely many diod blocks, each of which is either *trivial*, that is, the product of a segment and the 2-sphere with a finite number of disjoint 2-disks deleted, or *nontrivial*, that is, the complement, in the nontrivial segment bundle over the projective plane, of a finite number of trivial segment bundles over disjoint 2-disks. Choose a metric on the base of each diod block, for which a tubular neighborhood of each boundary circle is isometric to the product of a circle with an interval. All the boundary circles may be assumed to have the same length  $L$ . By rescaling, the sectional curvatures of these metrics may be assumed to satisfy  $|K| \leq 1$ . Then the metric on each diod block is taken to be locally a product with an interval of length  $\delta$ .

Finally we specify that for identity triod blocks, the interval  $I$  has length  $L$ , and for cyclic ones,  $I$  has length  $L/3$ . Equipping our blocks with these Riemannian

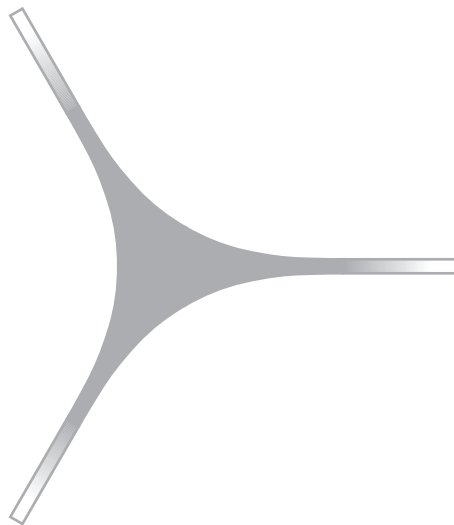


FIGURE 10.

metrics, and performing the gluings isometrically, converts our previous topological realizations into the required Riemannian ones.  $\square$

*Remark 5.3.* An analogous construction works in all dimensions to give spherical boundary components, provided there are no triod blocks with cyclic holonomy. Namely, we construct triod blocks with identity holonomy by multiplying the cross-section of Figure 10 by an  $(n - 2)$ -sphere with curvature less than 1. (This does not work for a triod block with cyclic holonomy, since the triod stratum of the spine will be  $S^{n-2}$ , whereas we need a triod stratum whose fundamental group has  $\mathbf{Z}_3$  as a quotient group.) The gluing seams of the triod blocks are products of  $S^{n-2}$  with an interval. For each diod block, we again use either a trivial segment bundle over the complement in  $S^{n-1}$  of disjoint  $(n - 1)$ -balls, or the complement in the nontrivial segment bundle over  $P^{n-1}$  of trivial segment bundles over disjoint  $(n - 1)$ -balls. Then each diod stratum of the boundary will be the complement of disjoint balls in  $S^{n-1}$ , and the gluing will realize each component of  $B$  as the connected sum of spheres. A Riemannian structure of the desired type fitting the topological realization just described does not require any special technique beyond what was used in the 3-dimensional case.

Now we consider the case  $n = 4$  in the presence of cyclic holonomy.

**Example 5.4.** We give an example of an admissible graph pair for which there is no 4-dimensional topological realization with  $H_1(B, \mathbf{Z}) = 0$ . Namely, consider Figure 4(c), which is the simplest pair with a cyclic triod vertex. For such a realization,  $B$  would be orientable. The triod stratum of  $B$  would be a closed orientable surface  $S$  triply covering the triod stratum of the spine, and hence  $S$  would have positive genus. The fact that there is only one diod block forces  $B$  to be the double of a 3-manifold  $\tilde{B}$  with boundary  $S$ . If  $H_1(B, \mathbf{Z}) = 0$ , then  $H_1(\tilde{B}, \mathbf{Z}) = 0$ . This is impossible, since the first Betti number of an orientable 3-manifold with boundary is at least the genus of the boundary [ST, §64].

**Example 5.5.** On the other hand, many graph pairs with cyclic triod vertices can be realized by a compact 4-dimensional manifold with spherical boundary components. Suppose the triod stratum  $C_{31}$  in the spine of a cyclic triod block is a torus. Then the lift  $B_{31}$  of that stratum is again a torus, which is the gluing seam between the two diod strata in the boundary that cover the diod stratum of the spine. To complete a desired realization, some further triod and diod blocks must be attached so as to fill a pair of generators of the first homology group of  $B_{31}$ . The graph pair in Figure 11 is sufficient, as we now verify.

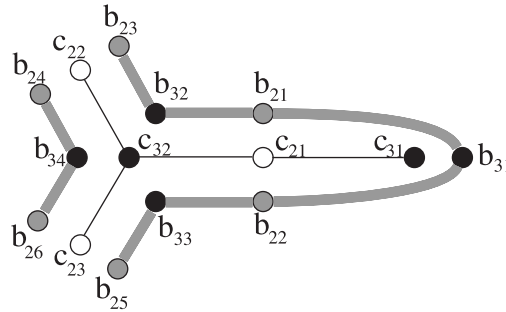


FIGURE 11.

We describe how to build a suitable spine, and then the structure of the boundary will be forced according to the graph. The diod stratum  $C_{21}$  will be taken to be a product  $T^2 \times I$ , of the torus  $T^2$  with an interval  $I$  (so the diod block over it will be a product with another interval). Take  $C_{32}$  to be  $T^2$  and the triod block over it to have identity holonomy. Then one end of  $C_{21}$  is glued to  $C_{32}$  by an arbitrary homeomorphism. Take  $C_{22}$  and  $C_{23}$  each to be a 3-sphere with a solid unknotted torus removed. Choose generators for  $H_1(C_{32}, \mathbf{Z})$  and glue the boundaries of  $C_{22}$  and  $C_{23}$  to  $C_{32}$  so that one generator can be filled by a disk in  $C_{22}$  and the other by a disk in  $C_{23}$ . Then both components of  $B$  will be 3-spheres, decomposed respectively by the torus gluing seams  $B_{34}$ , or  $B_{32}, B_{31}, B_{33}$ , in the same way that a Clifford torus, or a tubular neighborhood of it, respectively, decomposes the standard 3-sphere.

Again, a Riemannian metric realization fitting the topological realization just described would not require any special technique beyond what was used in the 3-dimensional case.

### 6. TOPOLOGICAL INVARIANTS

In this section we study further numerical invariants of compact  $n$ -dimensional manifolds  $M$  with triply branched simple polyhedral spines and simply connected boundary, and hence also for thin Riemannian manifolds with simply connected boundary. We do this by studying the invariants of admissible graph pairs  $(b, c)$ .

In addition to the invariants  $\ell, p, t, \beta, \gamma$  defined in §3.4, consider the following:

- $q$  = the number of diod vertices of  $c$ ,
- $r$  = the number of triod vertices of  $c$ ,
- $e$  = the number of edges of  $c$ .

There are other numerical invariants of the graph pair whose expression in terms of those already mentioned are clear. For instance, the number of diod vertices of  $c$  with  $\varphi$ -multiplicity 2 is  $q - p$ , and the number of triod vertices of  $c$  with  $\varphi$ -multiplicity 3 is  $r - t$ . The number of vertices of  $b$  is  $p + 2(q - p) + t + 3(r - t)$ . The number of edges of  $b$  is  $2e$ .

Note that in Theorem 4.1, the trivially covered diod and triod strata do not contribute visibly to the homeomorphism type, each of which typically is represented by many graph pairs. Nonetheless, we now show that the numbers of these strata (respectively,  $q - p$  and  $r - t$ ) are topological invariants. In our Riemannian setting, we have the somewhat surprising corollary that the numbers of diod and triod strata, respectively, of the cut locus are not merely geometric invariants of the Riemannian metric, but topological invariants of the underlying manifold.

**Theorem 6.1.** *All the above-mentioned numerical graph invariants of a finite admissible graph pair can be expressed in terms of  $\ell$ ,  $p$ ,  $t$ ,  $\beta$  and  $\gamma$ . Specifically,*

$$\begin{aligned} q &= 3\ell + 2p + 2t + 2\beta - 3\gamma, \\ r &= 2\ell + p + 2t + \beta - 2\gamma, \\ e &= 6\ell + 3p + 4t + 3\beta - 6\gamma. \end{aligned}$$

*Proof.* We start with the Euler characteristic equation for  $b$ :

$$\chi(b) = v - 2e = \text{rank } H_0(b) = \beta,$$

where  $v$  is the number of vertices of  $b$ , and  $2e$  is the number of its edges.

Since each triod vertex of  $c$  has valence equal to its multiplicity, the number of edges of  $c$  is  $e = t + 3(q - t)$ . The number of vertices of  $b$  is  $v = p + 2(r - p) + t + 3(q - t)$ . Therefore

$$p + 2(r - p) - t - 3(q - t) = \beta.$$

Now we calculate the Euler characteristic of  $c$  as we did for  $b$ :

$$\chi(c) = r + q - t - 3(q - t) = \text{rank } H_0(c) - \text{rank } H_1(c) = \gamma - \ell.$$

Now it is only necessary to solve the latter two equations for  $r$  and  $q$  in terms of the remaining variables.  $\square$

**Corollary 6.2.** *The number of diod and triod strata, respectively, of the cut locus of a thin Riemannian manifold  $M$  (of arbitrary dimension) whose boundary satisfies  $H_1(B, \mathbf{Z}) = 0$  depends only on the first homology of  $M$  and the number of components of  $M$  and  $B$ .*

*Proof.* By Theorem 3.4, the first homology of  $M$  determines  $\ell$ ,  $p$  and  $t$ . The number of components of  $M$  and  $B$  are  $\gamma$  and  $\beta$  respectively.  $\square$

**Example 6.3.** Figure 7 illustrates all admissible graph pairs having  $\ell = 1$ ,  $p = 1$ ,  $t = 0$ ,  $\beta = 1$  and  $\gamma = 1$ . Thus the figure shows all possible cut locus structures for a thin Riemannian metric on a manifold  $M$  with these topological invariants and  $H_1(B, \mathbf{Z}) = 0$ . The numbers  $q$  and  $r$  of the diod and triod strata are uniquely determined; in this case  $q = 4$ ,  $r = 2$ .

*Remark 6.4.* The graph pair calculus yields an algorithm for generating all admissible graph pairs, and hence all possible stratum structures for the cut loci of our thin Riemannian  $n$ -manifolds having (say) the invariant  $r$  at most equal to a given value  $k$ . Assuming  $\gamma = 1$ , this implies  $p + t + \ell + \beta \leq k + 2$  by Theorem 6.1. Copies

of Figure 4(a) or (b) will be called diod blocks, nontrivial or trivial respectively; their adjacent edges are as shown in Figure 3(c) or (d). Each of the following moves is performed in all possible ways on the members of a given family of graph pairs.

*Step 1.* Attach one copy of Figure 8(d) by identifying one of its ends with any trivial diod block (not necessarily an end). This move increases  $r$  and  $\beta$  by 1. Starting with an isolated trivial diod block, by  $k$  iterations generate  $k + 1$  families of admissible graph pairs with  $\ell = p = t = 0, \beta = r + 2 \leq k + 2$ .

*Step 2.* In a graph pair, choose two trivial diod blocks, one of which is an end, and which together intersect either three or four components of  $b$ . Identify them in both possible ways, unless they have a component of  $b$  in common; in that case there is only one way to identify them (that does not produce a loop in  $b$ ). This move preserves  $r$ , reduces  $\beta$  by 2 and increases  $\ell$  by 1. Starting with each family generated in the previous step, iterate at most  $\lfloor (k + 1)/2 \rfloor$  times.

*Step 3.* Choose a trivial diod block intersecting distinct components of  $b$ , and replace it with a nontrivial diod block. This preserves  $r$ , reduces  $\beta$  by 1, and increases  $p$  by 1. As before, iterate at most  $k + 1$  times.

*Step 4.* To a graph pair with  $r \leq k - 1$ , attach a copy of Figure 4(c) by identifying its end with any trivial diod block that intersects distinct components of  $b$ . This increases  $r$  by 1 and decreases  $\beta$  by 1. Iterate at most  $k + 1$  times.

All admissible graph pairs with  $r \leq k$  and  $\gamma = 1$  are generated, since for any such pair other than a trivial diod block, one of the operations inverse to those described is possible. This is clear if  $t > 0$  or  $p > 0$ , or if  $t = p = 0$  and  $\ell > 0$ . If  $t = p = \ell = 0$ , the spine graph is a tree whose ends are diod vertices, and removing these ends gives a tree whose ends are triod vertices. Such an end could only occur where the original had an attached copy of Figure 8(d), so an inverse of the first move is possible.

#### ACKNOWLEDGMENTS

We are very grateful to Wolfgang Haken for his helpful explanations and advice, and to Sergei Matveev for his helpful comments.

#### REFERENCES

- [AB1] S. B. Alexander, R. L. Bishop, *Thin Riemannian manifolds with boundary*, Math. Ann. **311**, 55–70 (1998). MR **99e**:53037
- [AB2] ———, *Spines and homology of thin Riemannian manifolds with boundary*, Advances in Math **155**, 23–48 (2000). MR **2002a**:53039
- [B] M. A. Buchner, *The structure of the cut locus in dimension less than or equal to six*, Compositio Math. **37** (1978), 103–119. MR **58**:18549
- [G] M. Gromov, *Synthetic geometry in Riemannian manifolds* in *Proceedings of the International Congress of Mathematicians, Helsinki, 1978* (O. Lehto, ed.), vol. 1, Adademia Scientiarum Fennica, 1980, 415–419. MR **81g**:53029
- [H] W. Haken, *Ein Verfahren zur Aufspaltung einer 3-Mannigfaltigkeit in irreduzible 3-Mannigfaltigkeiten*, Math. Zeitschr. **76** (1961), 427–467. MR **25**:4519c
- [I] H. Ikeda, *Acyclic fake surfaces which are spines of 3-manifolds*, Osaka J. Math. **9** (1972), 391–408. MR **50**:5800
- [K] H. Kneser, *Geschlossen Flachen in dreidimensionalen Mannigfaltigkeiten*, Jahresbericht der Deutschen Mathematiker Vereinigung **38**, 248–260 (1929).
- [LF1] V. Lagunov, A. Fet, *Extremal questions for surfaces of a given topological type*, Siberian Math. J. **4** (1963), 145–176. (Russian; English redaction by R. L. Bishop available on request). MR **27**:2918

- [LF2] ———, *Extremal questions for surfaces of a given topological type, II*, Siberian Math. J. **6** (1965), 1026–1036. (Russian; English translation by R. L. Bishop available on request). MR **33**:6555
- [MP] B. Martelli, C. Petronio, *Three-manifolds having complexity at most 9*, Experimental Math. **10** (2001), 207–236. MR **2002f**:57045
- [Ma1] S. V. Matveev, *Special spines of piecewise linear manifolds* Mat. Sb. (N.S.). **92** (134) (1972), 282–293; English translation in Math. USSR Sbornik **21** (1973). MR **49**:8027
- [Ma2] ———, *Complexity theory of three-dimensional manifolds*, Acta Applicandae Math. **19** (1990), 101–130. MR **92e**:57029
- [Ma3] ———, *Algorithmic Methods in 3-Manifold Topology*, (book to appear).
- [Mi] J.W. Milnor, *A unique decomposition theorem for 3-manifolds*, 1–7 (1961). MR **25**:5518
- [RS] C. Rourke, B. Sanderson *Introduction to Piecewise-Linear Topology*, Springer-Verlag, Berlin, Heidelberg and New York, 1982. MR **83g**:57009
- [ST] H. Seifert, W. Threlfall, *Lehrbuch der Topologie*, Teubner, Stuttgart, 1934; English translation, *A Textbook of Topology*, Academic Press, New York, 1980. MR **82b**:55001
- [Th] W. Thurston; Silvio Levy, Ed., *Three-Dimensional Geometry and Topology*, Volume 1, Princeton Univ. Press, Princeton, NJ, 1997. MR **97m**:57016
- [W] A. D. Weinstein, *The cut locus and conjugate locus of a riemannian manifold*, Ann. of Math. **87**, 29–41 (1968). MR **36**:4486

DEPARTMENT OF MATHEMATICS, UNIVERSITY OF ILLINOIS, 1409 W. GREEN ST., URBANA, ILLINOIS 61801

*E-mail address*: [sba@math.uiuc.edu](mailto:sba@math.uiuc.edu)

DEPARTMENT OF MATHEMATICS, UNIVERSITY OF ILLINOIS, 1409 W. GREEN ST., URBANA, ILLINOIS 61801

*E-mail address*: [bishop@math.uiuc.edu](mailto:bishop@math.uiuc.edu)